Molecular Cancer Therapeutics

Evaluation of Nonpeptidic Ligand Conjugates for the Treatment of Hypoxic and Carbonic Anhydrase IX–Expressing Cancers

Peng-Cheng Lv[1,2], Jyoti Roy[1,2], Karson S. Putt[1], and Philip S. Low[1,2]

Abstract

The majority of tumors contain regions of hypoxia, which cause marked phenotypic changes to resident cells. This altered gene expression often leads to increased resistance to anticancer treatments. Therefore, elimination of these resistant hypoxic cells is crucial to prevent disease recurrence. Herein, we describe the selective delivery of imaging and chemotherapeutic agents to cells expressing carbonic anhydrase IX (CA IX), a highly upregulated hypoxia receptor. These agents were conjugated to a potent divalent CA IX ligand through a hydrophilic PEG linker. These conjugates are shown to bind CA IX–expressing cells in a receptor-dependent manner *in vitro* with mid-nanomolar affinities and *in vivo* with good tumor selectivity. In a mouse xenograft tumor model using HT-29 cells, a cytotoxic tubulysin B conjugate completely inhibited tumor growth. Overall, the targeting of a hypoxia marker, such as CA IX, to selectively deliver imaging or chemotherapeutic agents may lead to better treatment options for solid, hypoxic tumors. In addition, the combination of standard chemotherapeutics that are most potent in normoxic dividing cells and drugs specifically designed to eliminate hypoxic nondividing cells may elicit a superior clinical outcome. *Mol Cancer Ther; 16(3); 453–60. ©2016 AACR.*

Introduction

Because of the defective formation of vasculature, the deposition of a dense extracellular matrix, and the insufficient assembly of lymphatic vessels, oxygen delivery to tumor tissues is often inadequate (1–3). While the extent of hypoxia can vary both temporally and spatially within a tumor (1–3), its clinical impact is almost always detrimental, with increases in chemoresistance, angiogenesis, radioresistance, metastasis, resistance to cell death, genomic instability, and the generation of cancer stem cells being the more common adverse consequences (4–7). Given the central contributions of these hypoxia-induced changes to tumor progression and survival, tumor hypoxia might well be considered one of the most important targets yet to be exploited in oncology.

Recent estimates suggest that 1% to 1.5% of all genes are hypoxia regulated (4). Thus, cells in hypoxic regions of tumors are commonly phenotypically different from normoxic cells, with some proteins increasing and others decreasing in abundance. In an effort to identify a hypoxia-induced protein that might be upregulated sufficiently in anaerobic cancers to be exploited for selective drug targeting, we searched for cell surface proteins that were dramatically induced by hypoxia yet absent or nearly absent in normoxic cells. The most prominent candidate to emerge from this search was carbonic anhydrase IX (CA IX), a membrane-spanning isoform of the intracellular carbonic anhydrases (8) that is significantly overexpressed in cancers of the lung (9), colorectum (10), stomach (11), pancreas (12), breast (13), cervix (14), bladder (15), ovaries (16), brain (17), head & neck (18), and kidneys (19). CA IX also appears to be upregulated on cancer cells on the edge of invasive tumors (20). In addition, CA IX is constitutively expressed in certain cancers, such as clear cell renal carcinomas where mutations in the *VHL* gene lead to continuous HIF-1α activation (19, 21, 22). Importantly, CA IX is absent from many healthy tissues (23), with high expression found only in the gastrointestinal tract and liver/gallbladder where most of the CA IX appears to be in a catalytically inactive form (23, 24). Low levels of CA IX can be found in skin (primarily hair follicles/sebaceous glands), testis, and salivary glands (23, 25).

Because of CA IX's cancer-enriched expression pattern, considerable effort has been expended to identify CA IX–specific ligands for use in tumor targeting. In fact, multiple CA IX ligands have been identified and conjugated to fluorophores (26–35), SPECT probes (34–48), and PET (49–59) agents with the goal of imaging hypoxic tumors. While therapeutic applications of some of these ligands have been explored in the literature, on the whole, less attention has been devoted to the important goal of eliminating malignant masses. Although an anti-CA IX antibody linked to a therapeutic radionuclide achieved only suppression of murine tumor xenograft growth (45), several small monovalent and bivalent CA IX ligands have shown much more promising results when coupled to cytotoxic drugs such as DM1 and duocarmycin (60, 61). Encouraged by these initial successes, we have undertaken to further explore the use of low molecular weight CA IX–targeting ligands to treat hypoxic tumors; only in this study, we

[1]Institute for Drug Discovery, Purdue University, West Lafayette, Indiana. [2]Department of Chemistry, Purdue University, West Lafayette, Indiana.

Note: Supplementary data for this article are available at Molecular Cancer Therapeutics Online (http://mct.aacrjournals.org/).

P.-C. Lv and J. Roy contributed equally to this article.

Corresponding Author: Philip S. Low, Department of Chemistry, Purdue University, 560 Oval Drive, West Lafayette, IN 47907. Phone: 765-494-5273; Fax: 765-494-5272; E-mail: plow@purdue.edu

doi: 10.1158/1535-7163.MCT-16-0537

have examined a different CA IX–specific ligand conjugated to an unrelated cytotoxic drug, tubulysin B.

Materials and Methods

Materials

Protected amino acids were purchased from Chem-Impex Intl. H-Cys (Trt)-2-Cl-Trt resin was obtained from Novabiochem. Tubulysin B and its activated derivatives were a kind gift from Endocyte Inc. 2-(1H-7-Azabenzotriazole-1-yl)-1,1,3,3-tetramethyl uronium hexafluorophosphate methanaminium (HATU) was obtained from Genscript Inc. Sulfuric acid, methanol, DMSO, DMF, TFA, isopropyl alcohol, NH_2-PEG_{12}-COOH-tBu, diisopropylethylamine (DIPEA), piperidine, CF_3COOH, CH_2Cl_2, K_2CO_3, tyramine, and all other chemical reagents were purchased from Sigma Aldrich. Purecoat Amine 24-well microtiter plates were purchased from BD Biosciences. All other cell culture reagents, syringes, and disposable items were purchased from VWR.

Synthesis of rhodamine conjugate

The CA IX ligand was prepared as described previously (62). For fluorescence imaging, the ligand was coupled with the rhodamine derivative (5-((5-aminopentyl)carbamoyl)-2-(6-(dimethylamino)-3-(dimethyliminio)-3H-xanthen-9-yl)benzoate hydrochloride) in the presence of EDC.HCl and HOBt in DMSO for 12 hours to yield the target conjugate. LRMS-LC/MS (m/z): $[M + H]^+$ calculated for $C_{52}H_{60}N_{10}O_{13}S_2$, 1,097.39; found, 1,097.

Synthesis of ^{99m}Tc conjugate

The radioimaging conjugate was synthesized by the following solid-phase methodology: H-Cys(Trt)-2-chlorotrityl resin (100 mg, 0.56 mmol/L) was swollen with 3 mL of dichloromethane (DCM) followed by 3 mL of dimethylformamide (DMF). For three times, a 3-mL solution of 20% piperidine in DMF was added to the resin with argon bubbled through for 5 minutes. The resin was washed three times with 3 mL of DMF and 3 times with 3 mL isopropyl alcohol (i-PrOH). After swelling the resin in DMF, a solution of Fmoc-Asp(tBu)-OH (2.5 eq), PyBOP (2.5 eq), and DIPEA (4.0 eq) in DMF was added. Argon was bubbled for 2 hours, and resin was washed three times with 3 mL of DMF and 3 times with 3 mL i-PrOH.

The above sequence was repeated for three more coupling steps for addition of Boc-DAP(Fmoc)-OH, Fmoc-NH-PEG_{12}-COOH, and CA IX ligand. The final compound was cleaved from the resin using a trifluoroacetic acid (TFA): H2O: tri-isopropylsilane: cocktail (95:2.5:2.5) and concentrated under vacuum. The concentrated product was precipitated in diethyl ether and dried under vacuum. Crude conjugate was purified by preparative RP-HPLC [A = 2 mmol/L ammonium acetate buffer (pH 7.0), B = CH_3CN, solvent gradient: 0% B to 100% B in 30 minutes] to yield the requisite product named CA IX-PEG_{12}-EC20. LRMS-LC/MS (m/z): $[M + H]^+$ calculated for $C_{59}H_{97}N_{11}O_{28}S_3$, 1503.57; found, 752.8 (half mass). For the L2-PEG_{36}-EC20 conjugate, LRMS-LC/MS (m/z): $[M + H]^+$ calculated for $C_{108}H_{195}N_{11}O_{52}S_3$, 2,574.21; found, 1,281.6 (half mass).

Synthesis of tubulysin B conjugate

CA IX–tubulysin B was synthesized from the CA IX–PEG_{12}–EC20 conjugate above. A solution of saturated sodium bicarbonate (2 mL) in HPLC grade water was bubbled with argon continuously for 10 min. CA IX-PEG_{12}-EC20 (50 mg, 0.033 mmol) was dissolved in argon-purged HPLC grade water (2.0 mL) and the pH of the reaction mixture was increased to 7 using argon purged sodium bicarbonate. A solution of disulfide activated-tubulysin B (37.47 mg, 0.034 mmol) in THF (2.0 mL) was then added to the reaction mixture. The progress of the reaction was monitored using analytic LC-MS, and after stirring for 30 minutes, the reaction was found to reach completion. Crude CA IX-tubulysin B was purified by preparative RP-HPLC [A = 2 mmol/L ammonium acetate buffer (pH 7.0), B = CH_3CN, solvent gradient: 0% B to 100% B in 30 minutes] to yield the requisite product. LRMS-LC/MS (m/z): $[M + H]^+$ calculated for $C_{104}H_{164}N_{18}O_{39}S_5$, 2,450.84; found, 1,225 (half mass).

Cell culture

HCT-116 (transfected with a CA IX expression vector), HT-29, RCC4, and SK-RC-38 human cancer cell lines were obtained from the ATCC in February 2015. No authentication was done by the authors prior to experimentation. All cells were cultured in RPMI1640 medium supplemented with 10% FBS and 1% penicillin–streptomycin at 37°C in a humidified 95% air–5% CO_2 atmosphere. Cells were split in an approximately 1:8 ratio when flasks reached confluence. All testing was performed by the 10th passage.

Fluorescent microscopy

HCT-116, HT-29, RCC4, and SK-RC-38 human cancer cell lines (10^5) were seeded into chambered coverglass plates and allowed to grow to confluence over 48–72 hours. Spent medium was replaced with 0.5 mL of fresh medium containing 0.5% BSA, and various concentrations of the dye conjugate alone or the dye conjugate plus 100-fold excess CA IX ligand. After incubation for 1 hour at 37°C, cells were rinsed with incubation solution (2 × 1.0 mL) to remove unbound conjugate then washed with PBS (1 × 1.0 mL). Images were acquired using confocal microscopy (FV 1000, Olympus).

^{99m}Tc conjugates and CA IX–rhodamine binding to HT-29 cells

HT-29 cells (150,000 cells/well in 500 μL) were seeded into 24-well Falcon plates and allowed to form monolayers over 48 hours. Spent medium in each well was replaced with 0.5 mL fresh medium containing increasing concentrations CA IX-PEG_{12}-EC20 bound with ^{99m}Tc or CA IX-rhodamine in the presence or absence of 100-fold excess CA IX ligand where appropriate. After incubating for 1 hour at 37°C, cells were rinsed twice with 1 mL of medium and 1 mL of Tris buffer. After dissolving in 0.5 mL of 0.25 mol/L NaOH (aq), for ^{99m}Tc conjugates, lysate was transferred into individual γ-counter tubes and radioactivity was counted using a γ-counter (Packard, Packard Instrument Company). For CA IX-rhodamine–treated cells, lysate was added to a quartz cuvette and fluorescence was measured in a fluorimeter. Apparent K_d was calculated by plotting bound radioactivity versus the concentration of radiotracer using GraphPad Prism 4.

Animal husbandry

Athymic nu/nu mice were purchased from Harlan Laboratories, housed in a sterile environment on a standard 12-hour light–dark cycle and maintained on normal rodent chow. All animal procedures were approved by the Purdue Animal Care and Use Committee in accordance with NIH guidelines.

^{99m}Tc conjugate biodistribution

Five-week-old male nu/nu mice were inoculated subcutaneously with HT-29 cells (5.0×10^6/mouse) on their shoulders. Growth of the tumors was measured in two perpendicular directions every 2 days using a caliper (body weights were monitored on the same schedule), and the volumes of the tumors were calculated as $0.5 \times L \times W^2$ (L = longest axis and W = axis perpendicular to L in millimeters). Once tumors reached between 400 and 500 mm^3 in volume, animals were administered ^{99m}Tc-bound conjugates (10 nmol, 150 μCi) in saline (100 μL) via tail vein injection. At various times, animals were sacrificed by CO_2 asphyxiation. Images were acquired after shielding the kidneys using a Kodak Imaging Station (In-Vivo FX, Eastman Kodak Company) in combination with CCD camera and Kodak molecular imaging software (version 4.0). For radioimages, illumination source = radio isotope, acquisition time = 3 minutes, *f*-stop = 4, focal plane = 5, FOV = 160, binning = 4. For white light images, illumination source = white light transillumination, acquisition time = 0.05 s, *f*-stop = 16, focal plane = 5, FOV = 160 with no binning. Following imaging, animals were dissected and selected tissues were collected to preweighed γ-counter tubes. Radioactivity of preweighed tissues and ^{99m}Tc-bound conjugates (10 nmol, 150 μCi) in saline (100 μL) was counted in a γ-counter. CPM values were decay corrected, and results were calculated as % injected dose (ID)/gram of wet tissue.

In vitro cytotoxicity of CA IX-tubulysin B

HT-29 cells were seeded on amine-coated 24-well plates and allowed to form monolayers. The spent medium in each well was replaced with fresh medium (0.5 mL) containing various concentrations of tubulysin B or CA IX-tubulysin B in the presence or absence of 100-fold excess CA IX ligand. After incubating for 1 hour at 37°C, cells were rinsed 3 times with fresh medium and then incubated an additional 24 hours at 37°C in fresh medium. Spent medium in each well was again replaced with fresh medium (0.5 mL) containing ^{3}H-thymidine (1 μCi/mL) and the cells were incubated for an additional 4 hours. After washing the cells three times with medium, they were dissolved in 0.5 mL of 0.25 mol/L NaOH. Thymidine incorporation was then determined by counting cell-associated radioactivity using a scintillation counter (Packard, Packard Instrument Company). The IC_{50} value was derived from a plot of the percent of ^{3}H-thymidine incorporation versus log concentration using Graph Pad Prism 4 and TableCurve 2D software.

MTD

Various concentrations of CA IX-tubulysin B were administered to male nu/nu mice thrice weekly via tail vein injection. Visibly sick mice were recorded and if necessary euthanized before the end of the experiment.

In vivo xenograft tumor efficacy of CA IX-tubulysin B

HT29 cells (5.0×10^6) were injected into the shoulders of 5- to 6-week-old female nu/nu mice. Tumors were measured in two perpendicular directions thrice weekly with vernier calipers and their volumes were calculated as $0.5 \times L \times W^2$, where L is the longest axis (in millimeters), and W is the axis perpendicular to L (in millimeters). Dosing of CA IX-tubulysin B in the presence or absence of 100-fold excess CA IX ligand was initiated when the subcutaneous tumors reached approximately 100 mm^3 in volume. Dosing solutions were prepared in saline and filtered through a 0.22-μm filter. Solutions were administered via tail vein injection or intraperitoneally. Each mouse received 2 μmol/kg CA IX-tubulysin B per injection. Injections were given thrice weekly for 3 weeks and the mice were weighed concurrently.

Results and Discussion

Synthesis and cellular uptake of CA IX–rhodamine conjugates

Ligand-targeted therapeutic agents are designed to selectively deliver imaging or therapeutic agents directly to the pathologic cells. The direct targeting of therapeutics typically reduces the efficacy as compared with the free drug; however, normal tissues are spared exposure leading to greatly reduced levels of toxicity. So, in an effort to identify ligands for use in targeting hypoxic tumors, a literature search for potent ligands of the hypoxia-induced cell surface enzyme, carbonic anhydrase IX (CA IX), was conducted. A suitable polyamino-polycarboxylamido aromatic sulfonamide ligand was chosen for conjugation (Fig. 1) due to its K_i of 7.8 nmol/L (62). In addition, the divalent nature of this molecule may aid in initial binding and internalization. Initially, this ligand was conjugated to a rhodamine via a five carbon alkyl chain to both explore the impact of conjugation on cellular binding and to ensure that the conjugate would bind to a variety of CA IX–expressing cancers. For this purpose, the CA IX–rhodamine conjugate was incubated with the CA IX–expressing cell lines HCT-116, HT-29, RCC4, and SK-RC-38 and examined by confocal microscopy. As shown in Fig. 2, binding is observed in every cell line tested, although HT-29 cells appeared to internalize the conjugate at a slower rate. To further assess binding, various concentrations of CA IX-rhodamine were incubated with HT-29 cells in the presence or absence of unbound ligand. The apparent K_d was found to be 105 nmol/L. Taken together, these data suggest that conjugation to one of the carboxylic acids does not markedly compromise binding. Importantly, when the fluorescent conjugate was incubated in the presence of 100-fold competing unconjugated CA IX ligand, essentially no binding was observed. This result shows that the binding is indeed receptor-mediated and that the conjugate was able to bind CA IX expressed on multiple different cell types (e.g., colon cancer and renal cell carcinomas). In addition, the punctate appearance of the fluorescence is indicative of internalization of the bound conjugate into endosomes during the 1-hour incubation period. This rapid uptake may be beneficial for the delivery of therapeutic agents.

Synthesis and cell binding of CA IX ^{99m}Tc conjugates

Once a suitable conjugation point was identified on the CA IX ligand, a PEG_{12} linker and ^{99m}Tc-binding moiety (EC20) were coupled to the ligand on the same carboxylic acid via the same amide reaction used for synthesis of the rhodamine conjugate (Fig. 1). The binding of this conjugate was saturable with an apparent dissociation constant of 54 nmol/L, and binding was successfully competed by addition of 100-fold excess free ligand. As the original ligand is reported to have a K_i of 7.8 nmol/L (62), the addition of the PEG_{12} linker and the ^{99m}Tc-binding moiety resulted in an approximately 7-fold loss of binding affinity. This loss of binding affinity is similar to other ligand-targeted conjugates we have synthesized and the overall affinity was deemed acceptable to move into *in vivo* studies.

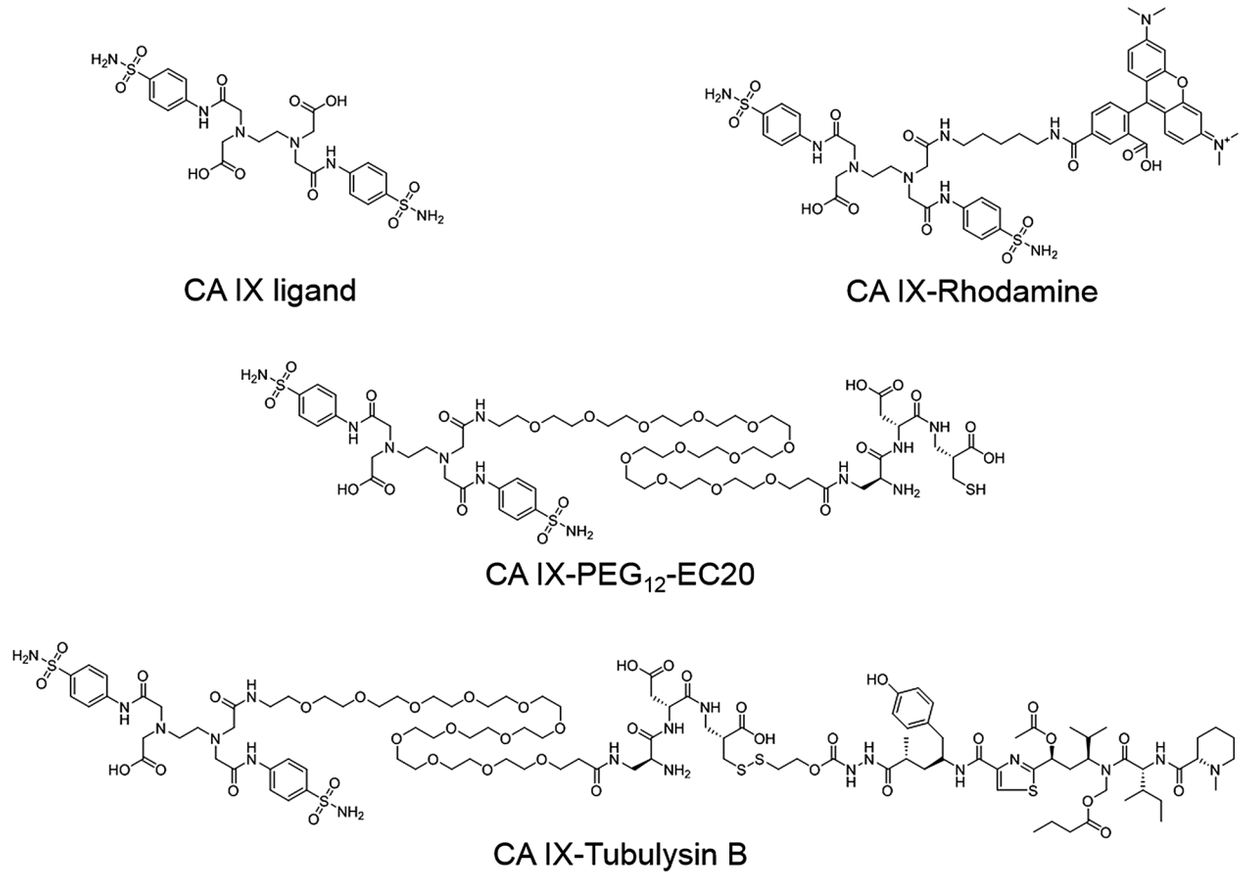

Figure 1.
Chemical structures of CA IX conjugates.

CA IX–specific uptake of CA IX ^{99m}Tc conjugates *in vivo*

Next, to determine whether the CA IX conjugate would specifically accumulate in CA IX–expressing tumors, a biodistribution was determined in mice bearing HT-29 xenografts. To accomplish this, 8 nmol of ^{99m}Tc-chelated conjugate was injected via the tail vein and mice were euthanized 4 or 22 hours later. The major organs/tissues were removed and the amount of radioactivity was determined. As shown in Fig. 3, the tumor exhibited the greatest percentage of injected dose (ID/g) at the 4-hour time point. Most of the uptake by the tumor was competed when 100-fold excess of unconjugated ligand was co-administered, showing that binding *in vivo* is also receptor mediated. In addition, the tumor was the only tissue that showed a statistically significant difference ($P = 0.038$) between the competed and non-competed groups at the 4-hour timepoint (Supplementary Fig. S1). The kidneys appear to be the primary route of excretion; however, signal in the intestine in the competition group may be due to some hepatic clearance as well. After 22 hours, the conjugate was nearly completely removed from all tissues including the tumor. Overall, these data support the fact that the CA IX–technetium conjugate specifically accumulates in the CA IX–expressing tumor.

When compared against several other CA IX–imaging agents, the accumulation within the tumor of this ^{99m}Tc-chelated conjugate is somewhat lower. For example, CA IX conjugates with the best BioD had uptake of 10%–20% ID/g in the tumor (34, 53, 54) at 4 hours. Other conjugates exhibited approximately 1%–5% ID/g (51) and a few poorly localized to the tumor with <1% ID/g (38, 39). Interestingly, the linker appears to play a large role in determining the biodistribution of polyamino-polycarboxylamido aromatic sulfonamide CA IX ligands. For example, when this ligand was coupled to longer PEG_{36} and semi-rigid $Proline_3$-PEG_{12} linkers, tumor uptake was approximately 5% ID/g (47). Why the linker has such an impact on this class of ligands is currently not known, but shows that exploring different linkers can be very important when optimizing the biodistribution of drug conjugates.

Synthesis and *in vitro* cytotoxicity of CA IX–tubulysin B conjugate

With receptor-mediated accumulation established in the tumor, the cytotoxic drug, tubulysin B, was conjugated to the sulfur of the CA IX-PEG_{12}-EC20 via a disulfide bond (Fig. 1). Tubulysin B, a natural product that inhibits tubulin polymerization was chosen due to its potent toxicity toward numerous cell lines (63). The long hydrophilic spacer was used to successfully block passive diffusion of the tubulysin B conjugate into non-targeted cells. To determine the cytotoxicity of this conjugate in a CA IX–dependent and independent fashion, first, CA IX-tubulysin B was incubated with HT-29 cells for 1 hour in the presence or absence of 100-fold unconjugated CA IX ligand. Then, cells were

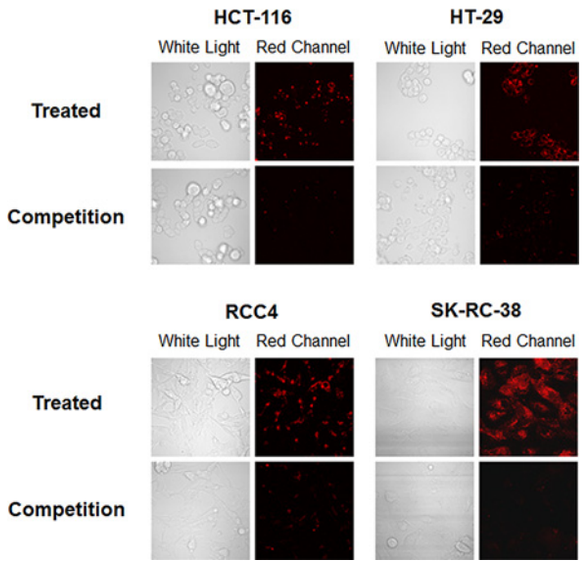

Figure 2.
In vitro binding of CA IX–rhodamine conjugate to various CA IX–expressing cell lines. The fluorescent CA IX–rhodamine conjugate (100 nmol/L) was incubated with various cell lines in the presence or absence of 100-fold excess free CA IX inhibitor (10 μmol/L). After washing, white light and fluorescent microscopy were used to visualize binding.

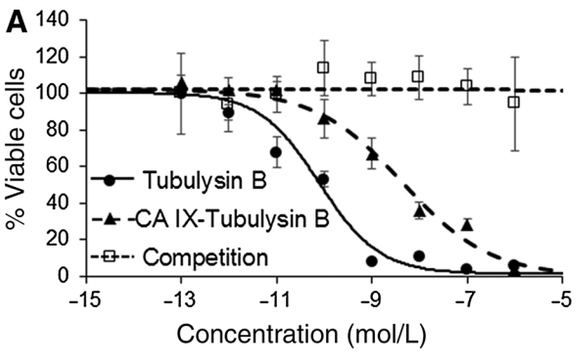

B

	Healthy	Sick	Euthanized
1 μmol/kg	3	0	0
3 μmol/kg	2	1	0
5 μmol/kg	0	1	2

Figure 4.
In vitro HT-29 cytotoxicity and *in vivo* MTD of CA IX-tubulysin B. **A,** Various concentrations of CA IX-tubulysin B with or without 100-fold excess CA IX inhibitor was incubated with HT-29 cells for 1 hour. After washing, the cells were incubated for 24 hours, and their viability was determined via ^{3}H-thymidine uptake. **B,** Healthy mice were administered CA IX-tubulysin B thrice weekly for 3 weeks. At the end of the third week, the numbers of healthy, visibly sick, and euthanized animals were recorded.

washed followed by a 24-hour incubation period. The number of viable cells was determined via ^{3}H-thymidine uptake. As shown in Fig. 4A, the IC_{50} value for the CA IX–targeted tubulysin B was 4.4 nmol/L. In contrast, when the targeted conjugate was competed with 100-fold excess of the free ligand, essentially no cytotoxicity was observed up to 1 μmol/L. The fact that free tubulysin B exhibited an IC_{50} value of 0.08 nmol/L suggests that little free drug was released prior to receptor-mediated uptake by the target cells. Taken together, these results demonstrate the requirement of receptor binding for cytotoxicity and the inability of the conjugate to passively diffuse through the cell membrane.

In vivo efficacy of CA IX-tubulysin B in mice bearing HT-29 xenografts

Prior to *in vivo* efficacy studies, a brief MTD study was performed. Three treatment groups consisting of 3 mice per group were administered increasing concentrations of CA IX-tubulysin B. As shown in Fig. 4B, no adverse events were observed when 1 μmol/kg CA IX-tubulysin B was administered. However, at the highest dose, 5 μmol/kg, all mice showed signs of toxicity. Therefore, a dose of 2 μmol/kg was used for all further *in vivo* efficacy studies. For evaluation of *in vivo* efficacy, 2 μmol/kg of drug was administered intraperitoneally or via tail vein injection every other day for 9 doses. As shown in Fig. 5, both administration routes essentially

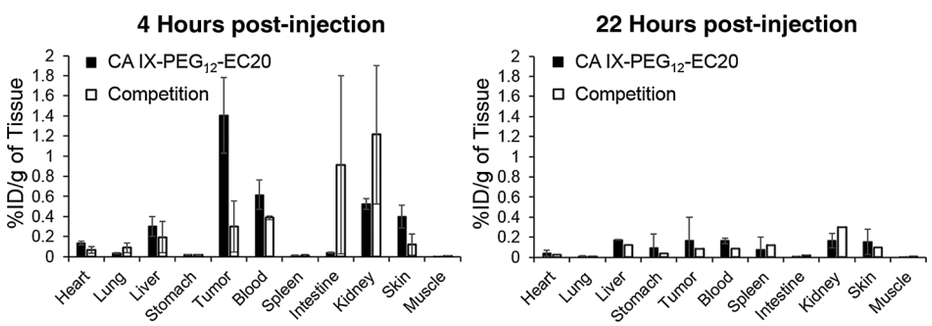

Figure 3.
In vivo biodistribution of CA IX-PEG_{12}-EC20. Nine mice bearing HT-29 xenograft tumors were administered 8 nmol ^{99m}Tc coordinated CA IX–Technetium conjugate via tail vein injection. An additional 9 mice were simultaneously injected with 100 nmol CA IX-PEG_{12}-EC20 and 10 μmol/L CA IX ligand. After 4 hours, 6 mice from each group were sacrificed. After an additional 18 hours (22 hours total), the remaining 3 mice from each group were sacrificed. Organs were excised, washed, weighed, and the amount of radioactivity present was determined. The percentage of the injected dose per gram (ID/g) of tissue was determined and plotted. Error bars, SD.

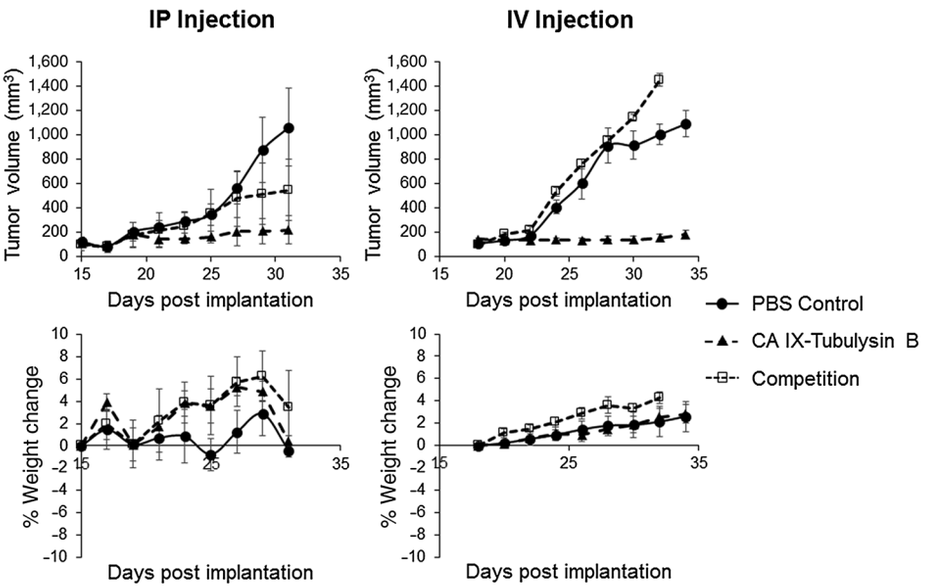

Figure 5.
In vivo efficacy of CA IX-tubulysin B. Mice were injected with 10^6 HT-29 cells. Once tumors reached a volume of approximately 100 mm^3, mice were randomized into various treatment groups ($n = 3$ for each IP and $n = 5$ for each IV group). CA IX-tubulysin B (2 μmol/kg) was administered intraperitoneally or via tail vein injection in the presence or absence of 100-fold excess CA IX ligand every other day for 9 total doses. Tumor volume and weight were measured every other day. Error bars, SEM.

halted growth of the HT-29 tumor xenografts while CA IX-tubulysin B is administered. As the tumor did not completely regress, cancer regrowth would likely occur once administration is halted in this mouse model. When the cytotoxic conjugate was administered in conjunction with 100-fold excess CA IX ligand, growth of the tumors was similar to that of the control group (statistical summary can be found in Supplementary Figs. S2 and S3). A free tubulysin B treatment group was not included in these experiments due to the known high toxicity of systemic administration of the free drug. These data demonstrate that the therapeutic efficacy *in vivo* is also mediated by CA IX–specific targeting. As no obvious toxicity was observed and no weight loss was detected, we conclude that this dosing level was both safe and effective in this murine tumor model (Fig. 5).

Conclusion

Because hypoxic regions of tumors are reported to harbor cells that are unusually difficult to eradicate (5–7), new strategies are required to assure that chemotherapeutic agents can reach these oxygen-depleted environments. Recognizing the strong upregulation of CA IX by hypoxia, the constitutive expression in certain cancer types, and presence on the leading edge of invasive tumors, we undertook to develop a CA IX–targeted drug that could concentrate in these more CA IX–enriched areas of a tumor. Data presented above reveal that the CA IX ligand identified here can indeed promote suppression of CA IX–expressing tumor growth when conjugated to the highly potent microtubule inhibitor, tubulysin B. It will now be important to find chemotherapeutic agents known to eradicate normoxic tumors that will most effectively synergize with this and other CA IX–targeted drugs.

Disclosure of Potential Conflicts of Interest

P.S. Low is a chief scientific officer at and reports receiving a commercial research grant from Endocyte, Inc. No potential conflicts of interest were disclosed by the other authors.

Authors' Contributions

Conception and design: P.-C. Lv, J. Roy, P.S. Low
Development of methodology: P.-C. Lv, J. Roy
Acquisition of data (provided animals, acquired and managed patients, provided facilities, etc.): P.-C. Lv
Analysis and interpretation of data (e.g., statistical analysis, biostatistics, computational analysis): P.-C. Lv, K.S. Putt
Writing, review, and/or revision of the manuscript: P.-C. Lv, J. Roy, K.S. Putt, P.S. Low
Administrative, technical, or material support (i.e., reporting or organizing data, constructing databases): P.-C. Lv
Study supervision: P.S. Low

Acknowledgments

The authors gratefully acknowledge the campus-wide mass spectroscopy facility and support from the Purdue University Center for Cancer Research (P30CA023168).

Grant Support

Funding for this project was made possible by a grant from Endocyte, Inc (to P.S. Low).

The costs of publication of this article were defrayed in part by the payment of page charges. This article must therefore be hereby marked *advertisement* in accordance with 18 U.S.C. Section 1734 solely to indicate this fact.

Received August 10, 2016; revised December 1, 2016; accepted December 5, 2016; published OnlineFirst December 15, 2016.

References

1. Noman MZ, Hasmim M, Messai Y, Terry S, Kieda C, Janji B, et al. Hypoxia: a key player in anti-tumor immune response. A review in the Theme: cellular responses to hypoxia. Am J Physiol Cell Physiol 2015; 309:C569–79.
2. Scanion SE, Glazer PM. Multifaceted control of DNA repair pathways by the hypoxic tumor microenvironment. DNA Repair 2015;32:180–9.
3. Harris BH, Barberis A, West CM, Buffa FM. Gene expression signatures as biomarkers of tumour hypoxia. Clin Oncol 2015;27:547–60.
4. Harris AL. Hypoxia – a key regulatory factor in tumour growth. Nat Rev Cancer 2002;2:38–47.
5. Yamada S, Utsunomiya T, Morine Y, Imura S, Ikemoto T, Arakawa Y, et al. Expressions of hypoxia-inducible factor-1 and epithelial cell adhesion

molecule are linked with aggressive local recurrence of hepatocellular carcinoma after radiofrequency ablation therapy. Ann Surg Oncol 2014; Suppl 3:S436–42.
6. Karakashev SV, Reginato MJ. Progress toward overcoming hypoxia-induced resistance to solid tumor therapy. Cancer Manag Res 2015;7:253–64.
7. DeClerck K, Elble RC. The role of hypoxia and acidosis in promoting metastasis and resistance to chemotherapy. Front Biosci 2010;15:213–25.
8. Pastorek J, Pastorekova S. Hypoxia-induced carbonic anhydrase IX as a target for cancer therapy: from biology to clinical use. Semin Cancer Biol 2015;31:52–64.
9. Ilie M, Mazure NM, Hofman V, Ammadi RE, Ortholan C, Bonnetaud C, et al. High levels of carbonic anhydrase IX in tumour tissue and plasma are biomarkers of poor prognostic in patients with non-small cell lung cancer. Br J Cancer 2010;102:1627–35.
10. Saarnio J, Parkkila S, Parkkila AK, Haukipuro K, Pastorekova S, Pastorek J, et al. Immunohistochemical study of colorectal tumors for expression of a novel transmembrane carbonic anhydrase, MN/CA IX, with potential value as a marker of cell proliferation. Am J Pathol 1998;153:279–85.
11. Chen J, Rocken C, Hoffmann J, Kruger S, Lendeckel U, Rocco A, et al. Expression of carbonic anhydrase 9 at the invasion front of gastric cancers. Gut 2005;54:920–7.
12. Juhasz M, Chen J, Lendeckel U, Kellner U, Kasper HU, Tulassay Z, et al. Expression of carbonic anhydrase IX in human pancreatic cancer. Aliment Pharmacol Ther 2003;18:837–46.
13. Tan EY, Yan M, Campo L, Han C, Takano E, Turley H, et al. The key hypoxia regulated gene CAIX is upregulated in basal-like breast tumours and is associated with resistance to chemotherapy. Br J Cancer 2009;100:405–11.
14. Loncaster JA, Harris AL, Davidson SE, Logue JP, Hunter RD, Wycoff CC, et al. Carbonic anhydrase (CA IX) expression, a potential new intrinsic marker of hypoxia: correlations with tumor oxygen measurements and prognosis in locally advanced carcinoma of the cervix. Cancer Res 2001;61:6394–9.
15. Klatte T, Seligson DB, Rao JY, Yu H, de Martino M, Kawaoka K, et al. Carbonic anhydrase IX in bladder cancer: a diagnostic, prognostic, and therapeutic molecular marker. Cancer 2009;115:1448–58.
16. Choschzick M, Oosterwijk E, Muller V, Woelber L, Simon R, Moch H, et al. Overexpression of carbonic anhydrase IX (CAIX) is an independent unfavorable prognostic marker in endometrioid ovarian cancer. Virchows Arch 2011;459:193–200.
17. Nordfors K, Haapasalo J, Korja M, Niemela A, Laine J, Parkkila AK, et al. The tumour-associated carbonic anhydrases CA II, CA IX and CA XII in a group of medulloblastomas and supratentorial primitive neuroectodermal tumours: an association of CA IX with poor prognosis. BMC Cancer 2010;10:148.
18. Hoogsteen IJ, Marres HA, Wijffels KI, Rijken PF, Peters JP, van den Hoogen FJ, et al. Colocalization of carbonic anhydrase 9 expression and cell proliferation in human head and neck squamous cell carcinoma. Clin Cancer Res 2005;11:97–106.
19. Liao SY, Aurelio ON, Jan K, Zavada J, Stanbridge EJ. Identification of the MN/CA9 protein as a reliable diagnostic biomarker of clear cell carcinoma of the kidney. Cancer Res 1997;57:2827–31.
20. Lloyd MC, Cunningham JJ, Bui MM, Gillies RJ, Brown JS, Gatenby RA. Darwinian dynamics of intratumoral heterogeneity: not solely random mutations but also variable environmental selection forces. Cancer Res 2016;76:3136–44.
21. Maxwell PH, Wiesener MS, Chang GW, Clifford SC, Vaux EC, Cockman ME, et al. The tumour suppressor protein VHL targets hypoxia-inducible factors for oxygen-dependent proteolysis. Nature 1999;399:271–5.
22. Stillebroer AB, Mulders PF, Boerman OC, Oyen WJ, Oosterwijk E. Carbonic anhydrase IX in renal cell carincoma: implications for prognosis, diagnosis, and therapy. Eur Urol 2010;58:75–83.
23. Uhlén M, Fagerberg L, Hallström BM, Lindskog C, Oksvold P, Mardinoglu A, et al. Tissue-based map of the human proteome. Science 2015;347: 1260419.
24. Pastorekova S, Parkkila S, Parkkila AK, Opavsky R, Zelnik V, Saarnio J, et al. Carbonic anhydrase IX, MN/CA IX: analysis of stomach complementary DNA sequence and expression in human and rat alimentary tracts. Gastroenterology 1997;112:398–408.
25. Syrjänen L, Luukkaala T, Leppilampi M, Kallioinen M, Pastorekova S, Pastorek J, et al. Expression of cancer-related carbonic anhydrase IX and XII in normal skin and skin neoplasms. APMIS 2014;122:880–9.
26. Wichert M, Krall N, Decurtins W, Franzini RM, Pretto F, Schneider P, et al. Dual-display of small molecules enables the discovery of ligand pairs and facilitates affinity maturation. Nat Chem 2015;7:241–9.
27. Dubois L, Douma K, Supuran CT, Chiu RK, van Zandvoort MA, Pastorekova S, et al. Imaging the hypoxia surrogate marker CA IX requires expression and catalytic activity for binding fluorescent sulfonamide inhibitors. Radiother Oncol 2007;83:367–73.
28. Dubois L, Lieuwes NG, Maresca A, Thiry A, Supuran CT, Scozzafava A, et al. Imaging of CA IX with fluorescent labelled sulfonamides distinguishes hypoxic and (re)-oxygenated cells in a xenograft model. Radiother Oncol 2009;92:423–8.
29. Bao B, Groves K, Zhang J, Handy E, Kennedy P, Cuneo G, et al. In vivo imaging and quantification of carbonic anhydrase IX expression as an endogenous biomarker of tumor hypoxia. PLoS One 2012;7:e50860.
30. Tafreshi NK, Bui MM, Bishop K, Lloyd MC, Enkemann SA, Lopez AS, et al. Noninvasive detection of breast cancer lymph node metastasis using carbonic anhydrases IX and XII targeted imaging probes. Clin Cancer Res 2012;18:207–19.
31. Ahlskog JK, Dumelin CE, Trussel S, Marlind J, Neri D. In vivo targeting of tumor-associated carbonic anhydrases using acetazolamide derivatives. Bioorg Med Chem Lett 2009;19:4851–6.
32. Groves K, Bao B, Zhang J, Handy E, Kennedy P, Cuneo G, et al. Synthesis and evaluation of near-infrared fluorescent sulfonamide derivatives for imaging of hypoxia-induced carbonic anhydrase IX expression in tumors. Bioorg Med Chem Lett 2012;22:653–7.
33. Lv PC, Roy J, Putt KS, Low PS. Evaluation of a carbonic anhydrase IX-targeted near-infrared dye for fluorescence-guided surgery of hypoxic tumors. Mol Pharm 2016;13:1618–25.
34. Muselaers CH, Rijpkema M, Bos DL, Langenhuijsen JF, Oyen WJ, Mulders PF, et al. Radionuclide and fluorescence imaging of clear cell renal cell carcinoma using dual labeled anti-carbonic anhydrase IX antibody G250. J Urol 2015;194:532–8.
35. Muselaers CH, Stillebroer AB, Rijpkema M, Franssen GM, Oosterwijk E, Mulders PF, et al. Optical imaging of renal cell carcinoma with anti-carbonic anhydrase IX monoclonal antibody girentuximab. J Nucl Med 2014;55:1035–40.
36. Muselaers CH, Stillebroer AB, Desar IM, Boers-Sonderen MJ, van Herpen CM, de Weijert MC, et al. Tyrosine kinase ligand sorafenib decreases 111In-girentuximab uptake in patients with clear cell renal cell carcinoma. J Nucl Med 2014;55:242–7.
37. Muselaers CH, Boerman OC, Oosterwijk E, Langenhuijsen JF, Oyen WJ, Mulders PF. Indium-111-labeled girentuximab immunoSPECT as a diagnostic tool in clear cell renal cell carcinoma. Eur Urol 2013;63:1101–6.
38. Akurathi V, Dubois L, Lieuwes NG, Chitneni SK, Cleynhens BJ, Vullo D, et al. Synthesis and biological evaluation of a 99m Tc-labelled sulfonamide conjugate for in vivo visualization of carbonic anhydrase IX expression in tumor hypoxia. Nucl Med Biol 2010;37:557–64.
39. Akurathi V, Dubois L, Celen S, Lieuwes NG, Chitneni SK, Cleynhens BJ, et al. Development and biological evaluation of 99mTc-sulfonamide derivatives for in vivo visualization of CA IX as surrogate tumor hypoxia markers. Eur J Med Chem 2014;71:374–84.
40. Li J, Shi L, Wang C, Zhang X, Jia L, Li X, et al. Preliminary biological evaluation of 125I-labeled anti-carbonic anhydrase IX monoclonal antibody in the mice bearing HT-29 tumors. Nucl Med Commun 2011;32: 1190–3.
41. Hendrickx BW, Punt CJ, Boerman OC, Postema EJ, Oosterwijk E, Mavridu A, et al. Targeting of biliary cancer with radiolabeled chimeric monoclonal antibody CG250. Cancer Biother Radiopharm 2006;21:263–8.
42. Honarvar H, Garousi J, Gunneriusson E, Höidén-Guthenberg I, Altai M, Widström C, et al. Imaging of CAIX-expressing xenografts in vivo using 99m Tc-HEHEHE-ZCAIX:1 affibody molecule. Int J Oncol 2015;46: 513–20.
43. Muselaers CH, Oosterwijk E, Bos DL, Oyen WJ, Mulders PF, Boerman OC. Optimizing lutetium 177-anti-carbonic anhydrase IX radioimmunotherapy in an intraperitoneal clear cell renal cell carcinoma xenograft model. Mol Imaging 2014;13:1–7.
44. Chrastina A, Závada J, Parkkila S, Kaluz S, Kaluzová M, Rajcáni J, et al. Biodistribution and pharmacokinetics of 125I-labeled monoclonal antibody M75 specific for carbonic anhydrase IX, an intrinsic marker of hypoxia, in nude mice xenografted with human colorectal carcinoma. Int J Cancer 2003;105:873–81.

45. Chrastina A, Pastoreková S, Pastorek J. Immunotargeting of human cervical carcinoma xenograft expressing CA IX tumor-associated antigen by 125I-labeled M75 monoclonal antibody. Neoplasma 2003;50:13–21.
46. Ahlskog JK, Schliemann C, Mårlind J, Qureshi U, Ammar A, Pedley RB, et al. Human monoclonal antibodies targeting carbonic anhydrase IX for the molecular imaging of hypoxic regions in solid tumours. Br J Cancer 2009;101:645–57.
47. Lv PC, Putt KS, Low PS. Evaluation of nonpeptidic ligand conjugates for SPECT imaging of hypoxic and carbonic anhydrase IX-expressing cancers. Bioconjug Chem 2016;27:1762–9.
48. Krall N, Pretto F, Mattarella M, Muller C, Neri D. A 99mTc-labeled ligand of carbonic anhydrase IX selectively targets renal cell carcinoma in vivo. J Nucl Med 2016;57:943–9.
49. Doss M, Kolb HC, Walsh JC, Mocharla VP, Zhu Z, Haka M, et al. Biodistribution and radiation dosimetry of the carbonic anhydrase IX imaging agent [(18)F]VM4-037 determined from PET/CT scans in healthy volunteers. Mol Imaging Biol 2014;16:739–46.
50. Hoeben BA, Kaanders JH, Franssen GM, Troost EG, Rijken PF, Oosterwijk E, et al. PET of hypoxia with 89Zr-labeled cG250-F(ab')2 in head and neck tumors. J Nucl Med 2010;51:1076–83.
51. Pan J, Lau J, Mesak F, Hundal N, Pourghiasian M, Liu Z, et al. Synthesis and evaluation of 18F-labeled carbonic anhydrase IX ligands for imaging with positron emission tomography. J Enzyme Inhib Med Chem 2014;29:249–55.
52. Pryma DA, O'Donoghue JA, Humm JL, Jungbluth AA, Old LJ, Larson SM, et al. Correlation of in vivo and in vitro measures of carbonic anhydrase IX antigen expression in renal masses using antibody 124I-cG250. J Nucl Med 2011;52:535–40.
53. Cheal SM, Punzalan B, Doran MG, Evans MJ, Osborne JR, Lewis JS, et al. Pairwise comparison of 89ZR- and 124I-labeled cG250 based on positron emission tomography imaging and nonlinear immunokinetic modeling: in vivo carbonic anhydrase IX receptor binding and internalization in mouse xenografts of clear-cell renal carcinoma. Eur J Nucl Med Mol Imaging 2014;41:985–94.
54. Divgi CR, Pandit-Taskar N, Jungbluth AA, Reuter VE, Gönen M, Ruan S, et al. Preoperative characterization of clear-cell renal carcinoma using iodine-124-labelled antibody chimeric G250 (124I-cG250) and PET in patients with renal masses: a phase I trial. Lancet Oncol 2007;8:304–10.
55. Minn I, Koo SM, Lee HS, Brummet M, Rowe SP, Gorin MA, et al. [64Cu]XYIMSR-06: a dual-motif CAIX ligand for PET imaging for clear cell renal cell carcinoma. Oncotarget 2016;7:56471–9.
56. Sneddon D, Niemans R, Bauwens M, Yaromina A, van Kuijk SJ, Lieuwes NG, et al. Synthesis and in vivo biological evaluation of (68)Ga-labeled carbonic anhydrase IX targeting small molecules for positron emission tomography. J Med Chem 2016;59:6431–43.
57. Peeters SG, Dubois L, Lieuwes NG, Laan D, Mooijer M, Schuit RC, et al. [(18)F]VM4-037 microPET imaging and biodistribution of two in vivo CAIX-expressing tumor models. Mol Imaging Biol 2015;17:615–9.
58. Lau J, Liu Z, Lin KS, Pan J, Zhang Z, Vullo D, et al. Trimeric radiofluorinated sulfonamide derivatives to achieve in vivo selectivity for carbonic anhydrase IX-targeted PET imaging. J Nucl Med 2015;56:1434–40.
59. Lau J, Zhang Z, Jenni S, Kuo HT, Liu Z, Vullo D, et al. PET imaging of carbonic anhydrase IX expression of HT-29 tumor xenograft mice with (68)Ga-labeled benzenesulfonamides. Mol Pharm 2016;13:1137–46.
60. Krall N, Pretto F, Neri D. A bivalent small molecule-drug conjugate directed against carbonic anhydrase IX can elicit complete regression in mice. Chem Sci 2014;5:3640–4.
61. Krall N, Pretto F, Decurtins W, Bernardes GL, Supuran CT, Neri D. A small-molecule drug conjugate for the treatment of carbonic anhydrase IX expressing tumors. Angew Chem Int Ed Engl 2014;53:4231–5.
62. Rami M, Winum JY, Innocenti A, Montero JL, Scozzafava A, Supuran CT. Carbonic anhydrase ligands: copper(II) complexes of polyamino-polycarboxylamido aromatic/heterocyclic sulfonamides are very potent ligands of the tumor-associated isoforms of IX and XII. Bioorg Med Chem Lett 2008;18:836–41.
63. Sasse F, Steinmetz H, Heil J, Hofle G, Reichenbach H. Tubulysins, new cytostatic peptides from myxobacteria acting on microtubuli. Production, isolation, physio-chemical and biological properties. J Antibiot 2000;53:879–85.